



Graphene as a flexible electronic material: mechanical limitations by defect formation and efforts to overcome

Seung-Mo Lee^{1,2}, Jae-Hyun Kim^{1,2,*} and Jong-Hyun Ahn^{3,*}

¹ Department of Nanomechanics, Nano-Convergence Mechanical Systems Research Division, Korea Institute of Machinery & Materials (KIMM), 156 Gajungbuk-ro, Yuseong-gu, Daejeon 305-343, Republic of Korea

² Nano Mechatronics, Korea University of Science and Technology (UST), 217 Gajeong-ro, Yuseong-gu, Daejeon 305-333, Republic of Korea

³ School of Electrical and Electronic Engineering, Yonsei University, 50 Yonsei-ro, Seodaemun-gu, Seoul 120-749, Republic of Korea

Defects in chemical vapor deposition (CVD) graphene seriously weaken its mechanical properties, and are harmful to other impressive physical properties. In particular, the poor mechanical properties of CVD graphene with defects are one of the most significant obstacles for graphene-based flexible electronics. In this mini-review, the types of defects in CVD graphene generated during the growth and handling stages are first briefly discussed. Then, the fracture behaviors of graphene with such defects are described. In addition, several effective methods for the direct or indirect early detection of those defects present in graphene are summarized. Lastly, recent studies to overcome these mechanical limitations induced by defects are introduced.

Introduction

The provisions of mechanical unrestrictedness, such as flexibility and stretchability, in electronics, can enable the possibility of various original applications, such as new types of displays, robotic sensory skins and biomedical devices. One of the most important requirements in the development of flexible (or stretchable) electronics is the simultaneous achievement of excellent mechanical deformability and electronic performance of the electronic component materials [1,2]. However, most inorganic-based electronic materials possess limited mechanical deformability compared with organic-based materials, restricting the range of flexible electronic applications.

In an effort to address such issues, new types of electronic materials have been intensively studied over the past decade. Specifically, graphene has attracted considerable attention as an alternative material to overcome the limitations of current inorganic-based electronic materials due to its excellent electronic and mechanical properties for flexible electronics [3], such as transistors [4], energy harvesting devices [5], photonic devices [6,7] and touch panels [8]. In particular, graphene grown by chemical vapor deposition (CVD) has mainly been studied for

practical applications because pristine graphene produced by mechanical exfoliation is of a limited size and difficult to fabricate [9,10]. However, CVD graphene possesses many defects, such as overlapped grain boundaries (GBs), pinholes and microcracks resulting from its synthesis, the catalytic metal etching process and the transfer processes. These defects seriously weaken its mechanical properties and decrease its other outstanding physical properties [11,12]. Thus, the poor mechanical properties of CVD graphene by defect formation are one of the most significant challenges for graphene-based flexible electronics.

In this article, the limitations of graphene's mechanical properties for flexible electronic applications and recent research progress to overcome its limitations will be reviewed. First, the types of defects in CVD graphene generated during synthesis and the transfer process, as well as their effect on the fracture of graphene and the failure of resultant devices, will be discussed. Then, effective methods to observe nano- and micro-sized defects in graphene using transmission electron microscopy (TEM), scanning tunneling microscopy (STM), atomic force microscopy (AFM) and other indirect techniques in combination with recent approaches to overcome limited mechanical properties through defect healing in graphene for flexible electronic applications will be explored.

*Corresponding authors: Kim, J.-H. (jaehkim@kimm.re.kr), Ahn, J.-H. (ahnj@yonsei.ac.kr)

Types of defects in graphene

The second law of thermodynamics (maximizing entropy (disorder)) explains the presence of defects in crystalline materials. Specifically, defects always exist in crystals, even in the thermodynamic equilibrium state. Such defects are usually regarded as imperfections in otherwise ideal materials, which could significantly influence the electrical, optical, mechanical properties of the material. Indeed, the mechanical characteristics, such as ductility, strength and fracture, of many technologically important materials, such as metals, are entirely governed by defects [13]. Although in some applications the defects could be exploited to alter the intrinsic physical properties of the materials to make them more useful and innovative, in general, the defects seriously degrade the mechanical performance of the materials. In many cases, increasing the defect density decreases the strength of the material.

Unlike defects in bulk materials that have a different dimensionality (0-D, 1-D, 2-D and 3-D), graphene has reduced dimensionality, which decreases the number of possible defect types, that is, point defects, line defects and GBs. Because of the sp^2 -hybridizing property of the graphene that allows the attachment of a varying number of nearest neighbor carbons, the carbon atoms themselves can form different polygon structures (not only hexagons but also pentagons, heptagons and octagons). This feature of graphene leads to the formation of nonhexagonal structures of carbon, that is, the simplest point defects (the Stone-Wales (SW) defects) [14]. The SW defects are caused by C–C bond rotation, which allows carbon polygons to switch between pentagons, hexagons and heptagons. Therefore, during the formation of the SW defects, no atoms are removed or added. The defects are simply created by the reconstruction of the graphene lattice. For instance, four

hexagons can be transformed into two pentagon–heptagon pairs (two pairs of 5–7 defects or SW (5577) defects) by rotating the C–C bond 90° , as depicted in Fig. 1a. Another simple defect form is vacancy, a missing atom in the graphene lattice (Fig. 1b and c). The mono- and di-vacancies have been experimentally visualized and characterized [15]. When considering a stable graphene with a perfect carbon lattice, every carbon atom is coordinated to three other carbon atoms. If many atoms are missing from the perfect graphene lattice, the defect configurations could become more complicated, and the graphene could be energetically unstable. If the number of missing atoms is even, the carbon atoms could be fully reconstructed, subsequently leaving no dangling bonds. By contrast, if an odd number of atoms are missing, there will be dangling bonds that render the graphene more unstable and reactive [16]. These dangling bonds could be adopted as useful sites to dope with impurities or functionalize with different atoms or molecules for other applications. However, the strong reactivity generally deteriorates the mechanical stability of graphene and accelerates fracture (the details will be covered in the next section).

The alignment of mono- and di-vacancy structures in graphene could form one-dimensional defects (Fig. 1d), that is, line defects, as already reported in many experimental studies [17–19]. These line defects are boundaries separating two independent domains of the different lattice orientation (Fig. 1e), which frequently appears in graphene grown on metal surfaces due to its simultaneous nucleation at different locations [20,21]. Metal surfaces with hexagonal symmetry are usually used to grow graphene by CVD. The symmetry mismatch between the metal and the graphene may lead to differing lattice orientations for different grains [22]. Therefore, the line defects corresponding to GBs in graphene could appear when two grains with different orientations coalesce.

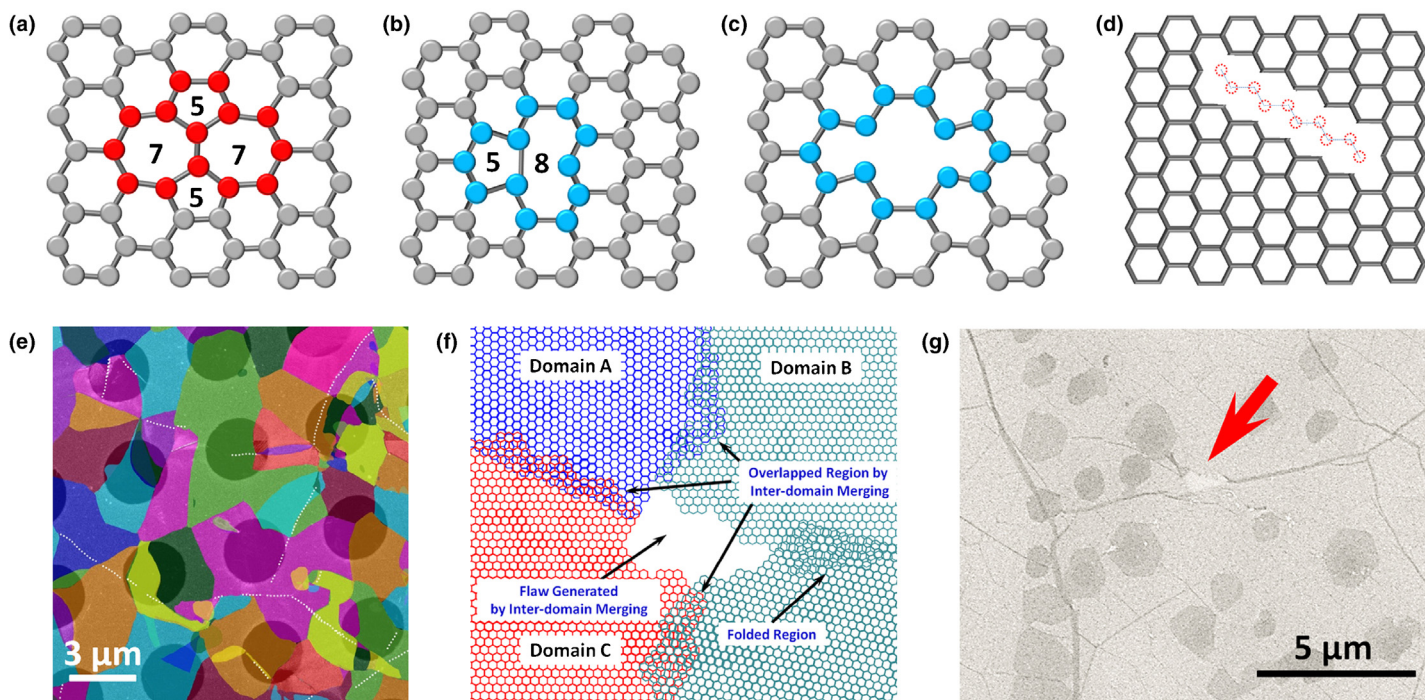


FIGURE 1

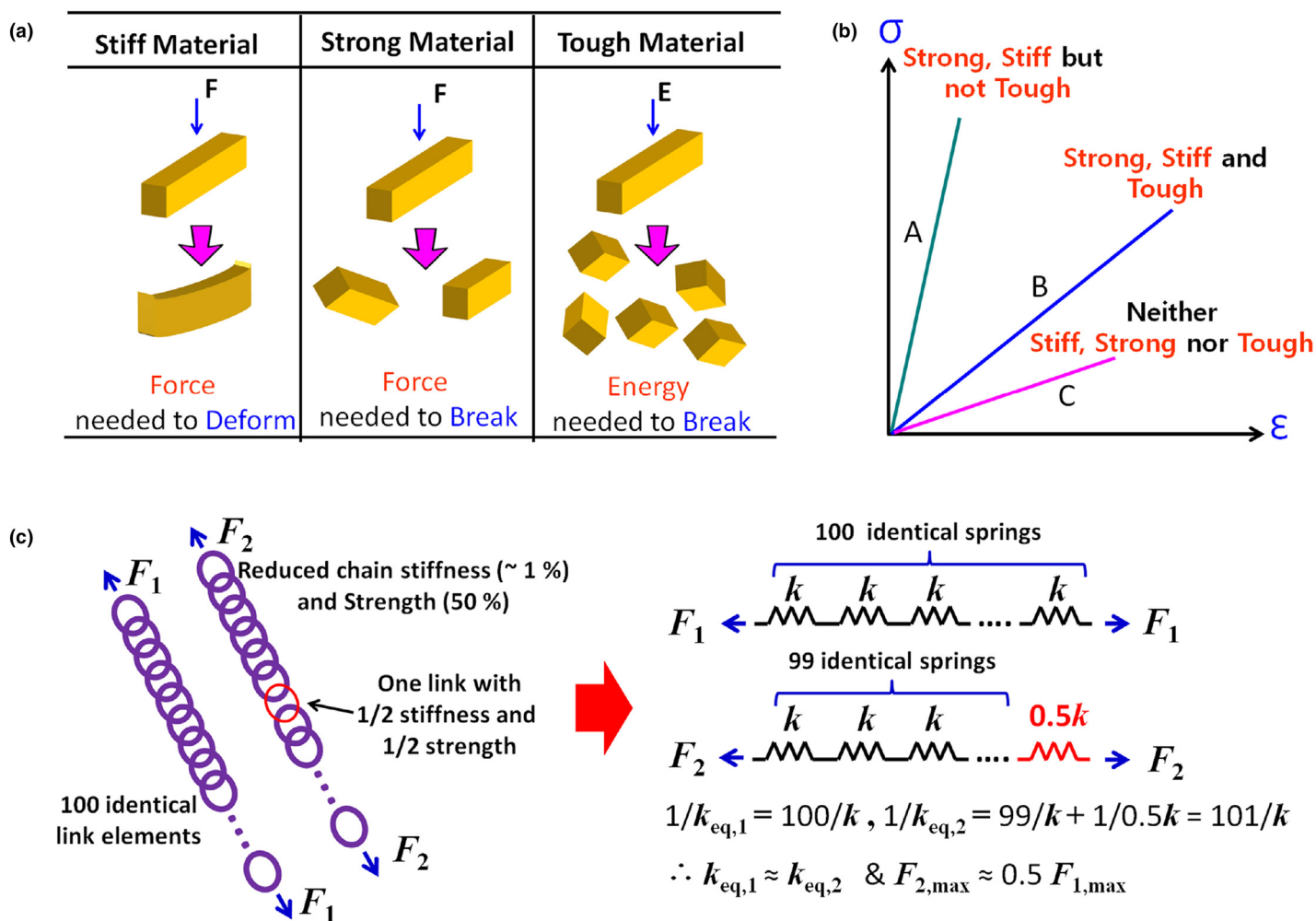
Defects in graphene. (a) Stone-Wales defect, SW (5577). (b) Mono-vacancy. (c) Di-vacancy. (d) Line defect formed by aligned vacancy structures. (e) Grain boundary mapping of polycrystalline CVD graphene. (f) Flaw generated by partial surface coverage of the CVD graphene. (g) Macroscopic defect created during the transfer processes.

Normally, graphene domains generated during CVD synthesis form nontrivial shapes, which largely depend on the growth conditions and can be rarely predicted beforehand. Therefore, in some cases, graphene grown on metal surface shows only partial surface coverage, thereby forming many areas with overlaps and small gaps (Fig. 1f) [23]. In addition, graphene can be easily damaged and torn during the transfer process, which could create macroscopic defects (Fig. 1g). Incontrovertibly, all defects are crucial for determining the properties of polycrystalline materials. Particularly, in graphene, defects have more pronounced effects, for example, even the line defects can divide and disrupt the crystals. The efforts to use graphene, particularly CVD-graphene, as a flexible electronic material have persisted in diverse fields. Although the electrical, optical and thermal properties of graphene determine the performance of graphene-based materials or devices, the mechanical properties largely represent the durability and reliability for practical uses. Clearly, the microscopic defects in particular vacancies, which inherently occur in the growth stage, significantly influence its mechanical behavior [12]. However, it should be reminded that the unwanted macroscopic defects that inadvertently occur during the handling stage

could be an absolute factor to decide the reliability of graphene-based materials and devices.

Fracture of graphene

It appears that the terms commonly used to describe the mechanical properties of certain materials, such as *stiff*, *strong* and *tough*, have been inappropriately overused, misrepresenting the actual conceptual differences between them (Fig. 2). The *stiffness*, k ($k = F/\delta$, where F and δ are the applied force and the produced displacement, respectively), of a material quantifies resistance against deformation when it is subjected to an applied force. In general, stiffness is not identical with the *elastic modulus*, E ($E = \sigma/\varepsilon$, where σ and ε are the applied stress and the produced strain, respectively), although stiffness is proportional to the elastic modulus (i.e. $k = (A/L)E$, where A and L are the cross-sectional area and the length of the element, respectively). *Strength* is defined as the maximally sustainable stress before breaking. Therefore, high strength allows carrying high load, and many structural materials are usually simultaneously stiff and strong. In the presence of defects, there is an essential difference in how these two properties are influenced. Presumably, this difference can be roughly understood by the weak link problem depicted in



Weak Link Problem

FIGURE 2

(a) Mechanical characteristics of materials: *stiffness*, *strength* and *toughness*. (b) Stress–strain curves of different mechanical characteristics. (c) Weak link problem.

Fig. 2. Given that one of 100 identical links in a chain has half stiffness and half strength, the overall stiffness of the chain is reduced by just $\sim 1\%$; however, the strength is measurably reduced by half. This effect implies that small defects hardly influence the stiffness; however, the strength is seriously influenced by the defects. The term *toughness*, which is related to the energy required to propagate a crack through the material and finally to break it, rather differs from the other two parameters. Toughness is estimated by the area under the stress–strain curve until failure. This area demonstrates the energy per volume that the material can absorb before rupturing. A better definition can be given in terms of the energy per unit crack area. This energy required to elongate a pre-existing crack is called the critical energy release rate ($G_C, \text{J/m}^2$). The quantity, $K_{Ic} = (EG_C)^{1/2}$ (critical stress intensity factor (SIF) or critical strain energy release rate at the moment of crack extension), is usually defined as *fracture toughness*, which is widely accepted as a benchmark describing the ability of a material containing inherent flaws or defects to resist fracture.

Several experimental studies on the mechanical properties of graphene have been reported up to date. These studies have mainly focused on the elastic modulus and strength [12,24,25]. Indeed, the elastic modulus and strength could be important concepts for understanding the general mechanical behavior of

graphene. However, in engineering, identifying general fracture behaviors of graphene in the presence of defects or flaws is of paramount importance rather than exploring the elastic modulus and strength, which are related to the uniform deformation or the rupture of carbon bonds. Because of the extreme difficulty in preparing graphene samples for the observation of fracture behaviors, relevant experimental studies have been rare [26,27]. In a recent work, Hwangbo et al. [27] reported for the first time the real time fracturing process of monolayer CVD graphene. After preparing suspended graphene membranes on perforated substrates (Fig. 3a and b), the membranes were mounted on a bulge test apparatus equipped with a synchronized high-speed camera (Fig. 3c). As the pressure difference (ΔP , in room conditions) gradually increases, the crack in the CVD graphene grows in a discontinuous and complicated manner (Fig. 3d) followed by catastrophic failure within a time of less than 2 ms ($A \rightarrow B$). Notably, the crack arrest and re-initiation processes occur repetitively, as can be recognized from the crack growth rate curves (Fig. 3e). For instance, from t_2 to t_4 , the crack does not propagate, and the corresponding captured images hardly show any perceivable variations in the crack length extension. Because graphene consists of a uniform carbon-based 2D monolayer, the retardation of the propagating crack by certain growth inhibitors

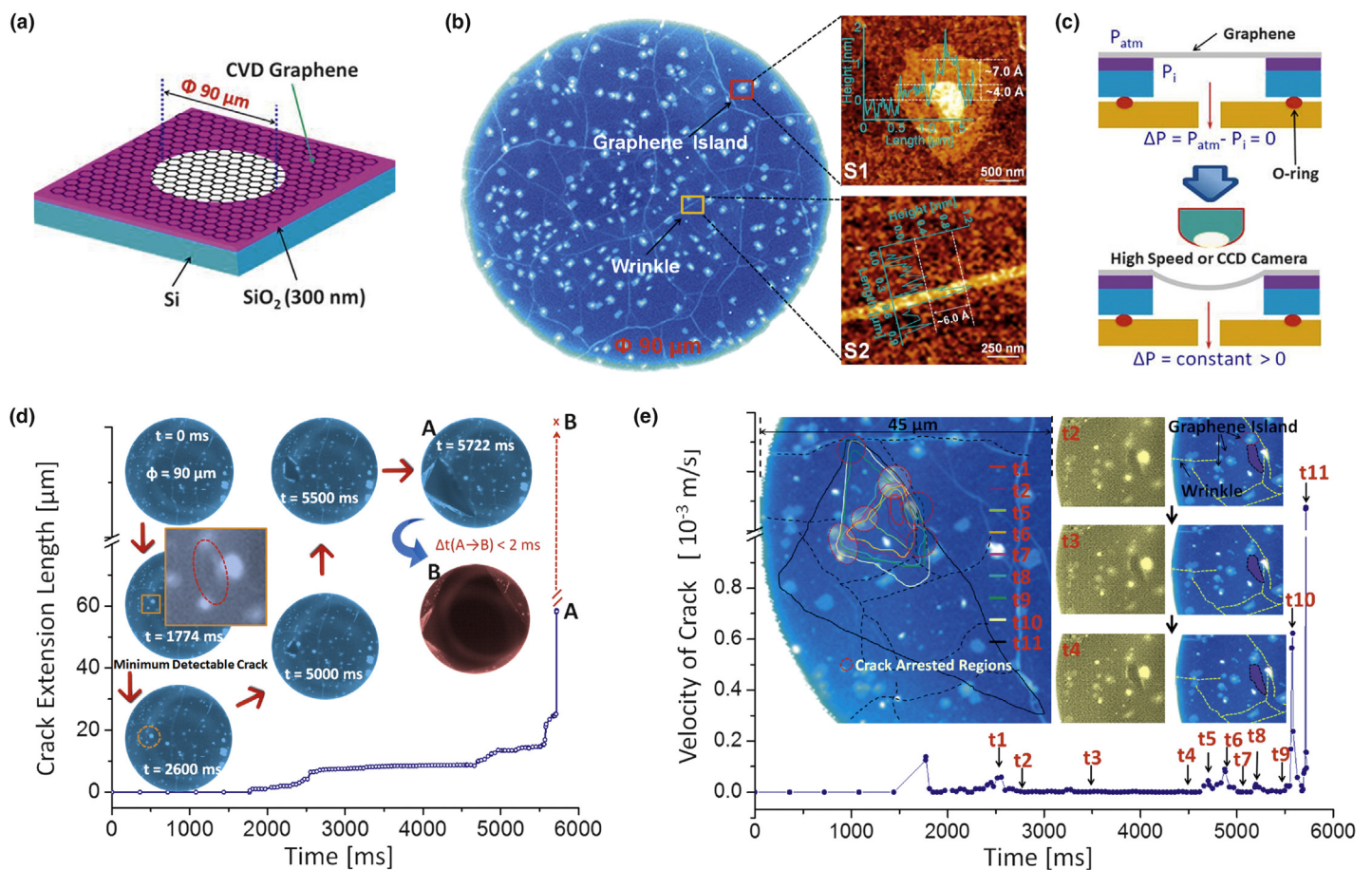


FIGURE 3

(a) Schematic of freely suspended CVD graphene on a Si substrate with a cylindrical hole. (b) Optical microscope image of the suspended monolayer graphene with wrinkles and graphene islands, and contact mode atomic force microscope (AFM) images of graphene with wrinkles and islands. (c) Schematic illustration of the bulge test setup. (d) Crack extension history with typical images showing fracture evolution. (e) Crack propagation speed diagram. The inset pictures show crack-arresting behaviors arising from thickness differences. Adapted from Ref. [27].

can be intuitively regarded as a less probable phenomenon. However, it resulted that the thick graphene islands and wrinkles (Fig. 3b) existing on the CVD graphene were the main crack arrestors, thereby preventing abrupt crack propagation and extending the lifetime of the CVD graphene.

When bulk materials such as metals are exposed to corrosive environments and subjected to tensile stress, the material often experiences unexpected sudden failures. Cracks can initiate and propagate well below the critical SIF (K_{Ic}). This failure, accompanying subcritical crack growth, is referred to as stress corrosion cracking (SCC). SCC typically shows a tri-modal behavior in the diagram, which shows the relationship between the SIF (K) and the crack velocity (V) [28,29]. Surprisingly, the CVD graphene experiences SCC under ambient conditions (Fig. 4). This result means that although its fracture toughness is comparable to diamond, it can be subjected to early failure once it is under the combined influence of tensile stress and a corrosive environment. As mentioned above, the dangling bonds induced by the formation of point, line, GB and macroscopic flaws surely allow the reactions between carbon bonds and molecules, such as H_2O , H_2 , CO_2 , NH_3 , O_2 , among others [30–32]. These adsorbates have an effect on the physical/chemical properties of graphene, which leads to new physico-chemical properties and, more importantly, induce configuration changes caused by orbital hybridization from a planar sp^2 -hybridized geometry to a distorted 3D sp^3 -hybridized geometry by charge transfer. Hydrogenation (sp^3 , C–H bond) [33] and the folding/unzipping of graphene by the formation of an oxidation-induced epoxy group (–O–) in graphene [34] are typical examples. The molecules existing in the atmosphere create bonds (such as C–H, C–OH, or C–O–C) on the graphene defects, thereby inducing configuration changes from a 2D sp^2 geometry to a 3D sp^3 geometry. Once the external load is applied to the distorted graphene, the initiated or pre-existing cracks propagate, producing fracture lines with further numerous dangling bonds on the graphene. On those dangling bonds, hydrogen and oxygen readily create new bonds,

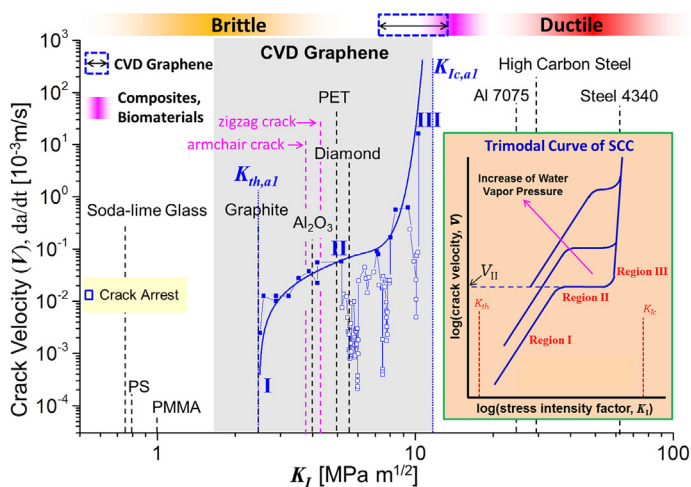


FIGURE 4

Stress intensity factor (K_I) versus crack velocity (or growth rate, $V = da/dt$) diagram for CVD graphene in ambient conditions. A comparison of the measured or calculated fracture toughness (K_{Ic}) values between the CVD graphene and widely known materials is summarized. The data points marked with an open square (blue) denote ($V - K_I$) values associated with crack arresting. The inset shows a typical tri-modal curve of stress corrosion cracking. Adapted from Ref. [27].

leading to further changes in the configuration. These cyclic processes result in further crack initiation/propagation triggered by the external load before reaching catastrophic failure.

Most graphene-based flexible materials and devices are established on the premise that they can be used in environmental conditions, except for few specific applications. Although graphene is impressively stiff and strong, its fracture characteristics are below expectations for emerging applications. Currently, many graphene-based flexible devices employ polymer substrates. Because most polymers swell in water, the polymer substrate could function as a water reservoir for the graphene in the worst case. Consequently, the polymer most probably leads to unwanted abrupt fractures arising from SCC and the extreme water sensitivity of defective graphene [27]. Therefore, encapsulation and defect healing issues would be the most pressing problems to solve.

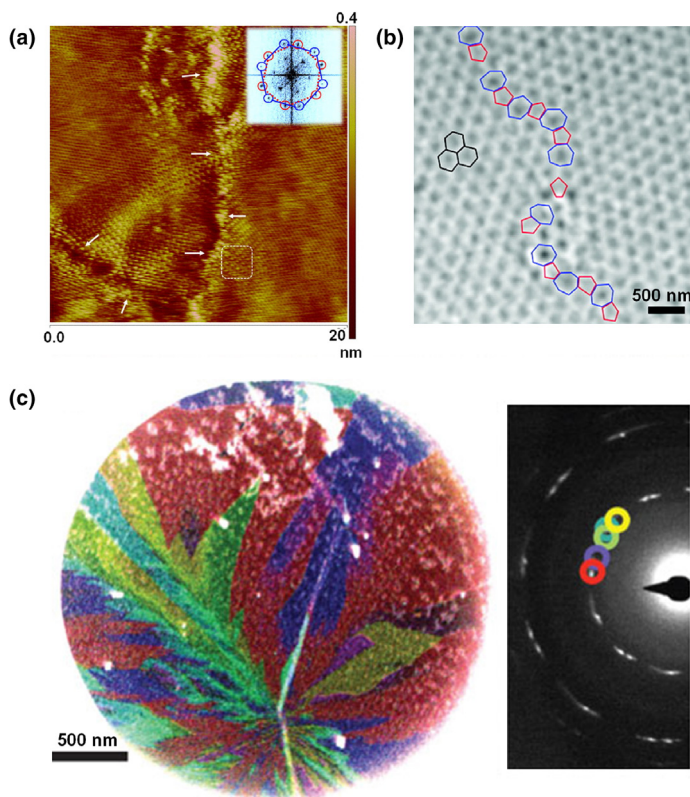
Observation of defects in graphene

Various defects in large-area CVD graphene, which are mainly created during the growth and the transfer processes, degrade the initial quality of graphene required for electronic devices and lead to the failure of devices. Therefore, it is important to thoroughly observe the distribution of defects in graphene and fully understand the generation mechanisms of defects during each step. In particular, it is necessary to understand the growing problem of defects generated in graphene under high strain for its use in flexible and stretchable electronic devices.

The physical properties of CVD graphene are strongly dependent on the distribution and the density of its defects. A variety of approaches have been explored to clearly observe the defects and the GBs in graphene. They can be classified into two general approaches: one that indirectly observes the existence of defects in graphene using Raman spectroscopy [35] and another that makes a direct observation of defects using microscopic tools. The latter approach is more attractive because it is possible to specifically and directly observe a variety of defects in large-area graphene. This approach can technically be divided into two categories according to the use of an additional process that enhances signal detection in defects: one that directly views the defects of graphene over a small area of (nano ~ micrometer scale using TEM [19,36] and STM [37] (Fig. 5)) and another that observes the defects using optical microscopy or AFM after selective oxidation of a defect region [38,39] or anisotropic alignment of the liquid crystal (LC) molecules over a large area of graphene [40,41] (Fig. 6).

STM has been applied to observe the point and line defects in graphene. This method can provide very clear atomic-resolution images of various defects in graphene (Fig. 5a). However, the atomic-resolution image of the defects is perturbed by a substrate, which is a disadvantage of this surface probe technique for the fundamental understanding of the physical properties of defects. Huang et al. [19] and Kim et al. [36] successfully directly mapped grain images and GBs of polycrystalline graphene sheets at the several micrometer scale using electron diffraction in scanning transmission electron microscopy (STEM) and dark-field imaging in TEM (Fig. 5b and c). The method revealed that the grains have many different crystal orientations, and the GBs are composed of complex shapes.

However, these microscopic tools have several drawbacks including the complexity of sample preparation, the observation

**FIGURE 5**

(a) Atomic-resolution STM image of polycrystalline graphene revealing linear defective features corresponding to grain boundaries. (b) Magnified image of the high-angle tilt grain boundary of graphene. The pentagon, hexagon and heptagon are overlaid with red, black and blue polygons, respectively. The GB shows an array of alternating pentagon and heptagon structures. (c) Low magnification image of grains by dark-field TEM. Adapted from Refs. [19,36,37].

time-delay to be followed and a limited observation area range. To resolve such drawbacks, alternative methods have recently been demonstrated. Nemes-Incze et al. [38] reported an approach to observe the GBs in graphene by AFM after the selective oxidation of defects. Oxidation can enhance the contrast between the grain and the GB because the reaction rate with moisture of the atoms in GBs is relatively faster than the stable atoms in grains. (Fig. 6a and b) This method can quickly and simply analyze the defects and grain size distribution in graphene. In a similar way, selective oxidation of the underlying copper foil through GBs of graphene functionalized with radicals make the volume of copper expand such that the GBs can be optically distinguished (Fig. 6c).

Alternatively, an effective method based on the properties of LC molecules, which anisotropically align along the graphene domain orientations, was recently reported [40,41]. LC molecules preferentially align according to the anisotropy of graphene grains, and thereby the exact shape of graphene grains becomes visible (Fig. 6d). In addition, the defects and crack propagation in graphene were visualized by observing phase transitions in a LC mixture due to the interactions of each constituent molecule of the LC mixture with an underlying polydimethylsiloxane (PDMS) substrate. This observation method offered unique advantages in terms of rapid imaging and the ability to identify domains in a large-area graphene film without complicated sample preparation

processes. In addition, this method allowed the observation of the defect generation process in a graphene film under external strain.

Methods to overcome defects in graphene for real applications

As strongly emphasized in the previous section, the microscopic and macroscopic defects in graphene originate from the growth and transfer stages, significantly degrading its electronic performance and causing poor fracture characteristics. To reduce the defect density in the graphene, developing precisely controlled growth and transfer methods would be a promising solution.

In general, reducing the nucleation seed density on a metal catalyst or/and aligning the orientation of seeds in the initial stage of CVD growth are crucial processes for growing graphene with a low defect density to meet the requirements for graphene-based electronic devices. A pre-annealing method for achieving large grains and a smooth surface of Cu foils, preventing Cu from evaporating from the foil surface during the growth step, and maintaining a Cu_2O layer on the Cu foil surface have been reported to suppress the nucleation density to grow large, single crystal graphene [42–44]. Recently, Lee et al. reported a promising method to grow wafer-scale single crystal graphene on Si wafers using a Ge semiconductor as a catalyst [45]. Multiple nucleation seeds in the initial stage were unidirectionally aligned by the anisotropic twofold symmetry of the Ge (1 1 0) surface. Multi-grains with uniform orientation were then finally merged to form a single grain without line defects similar to a GB.

In an effort to transfer graphene grown by the CVD process to foreign, useful substrates without additional defect creation, various transfer approaches have been investigated. Song et al. demonstrated a self-releasing method that enables the transfer of large-area graphene onto a variety of surfaces [46]. In this method, a self-releasing polymer layer is inserted between the elastomeric stamp and the graphene film. The low adhesive force between the stamp and the inserted polymer allows graphene coated with polymer to softly transfer to a target substrate, avoiding bending stresses that can cause the graphene film to fracture. Recently, a unique approach based on electrostatic forces without using an additional organic support was reported [47]. A target substrate accumulated with electrostatic charges gently attaches to the graphene on Cu foil, and the foil is then removed using a wet etchant. The method facilitates the transfer of large-area graphene without an organic residue.

In addition, the development of unconventional and smart methods for defect healing is also required because the formation of inherent defects is unstoppable. Various approaches based on molecular-dynamic simulations have been reported to heal the defects in graphene. Karoui et al. reported that the graphene defects on a metallic substrate such as Ni could be healed through thermal annealing. The direct interaction between the metal and carbon required for healing is created around the defected carbon region and thereby reforms the defected carbon bonds [48]. Moreover, Wang and Pantelides demonstrated that graphene vacancies could be healed by exposure to gases such as CO and NO. A CO gas molecule is placed at a vacancy site, and then a NO molecule removes the extra O by forming NO_2 [49].

In an experimentally based approach, Lam et al. investigated the strong reactivity of the dangling bonds of the defects and the

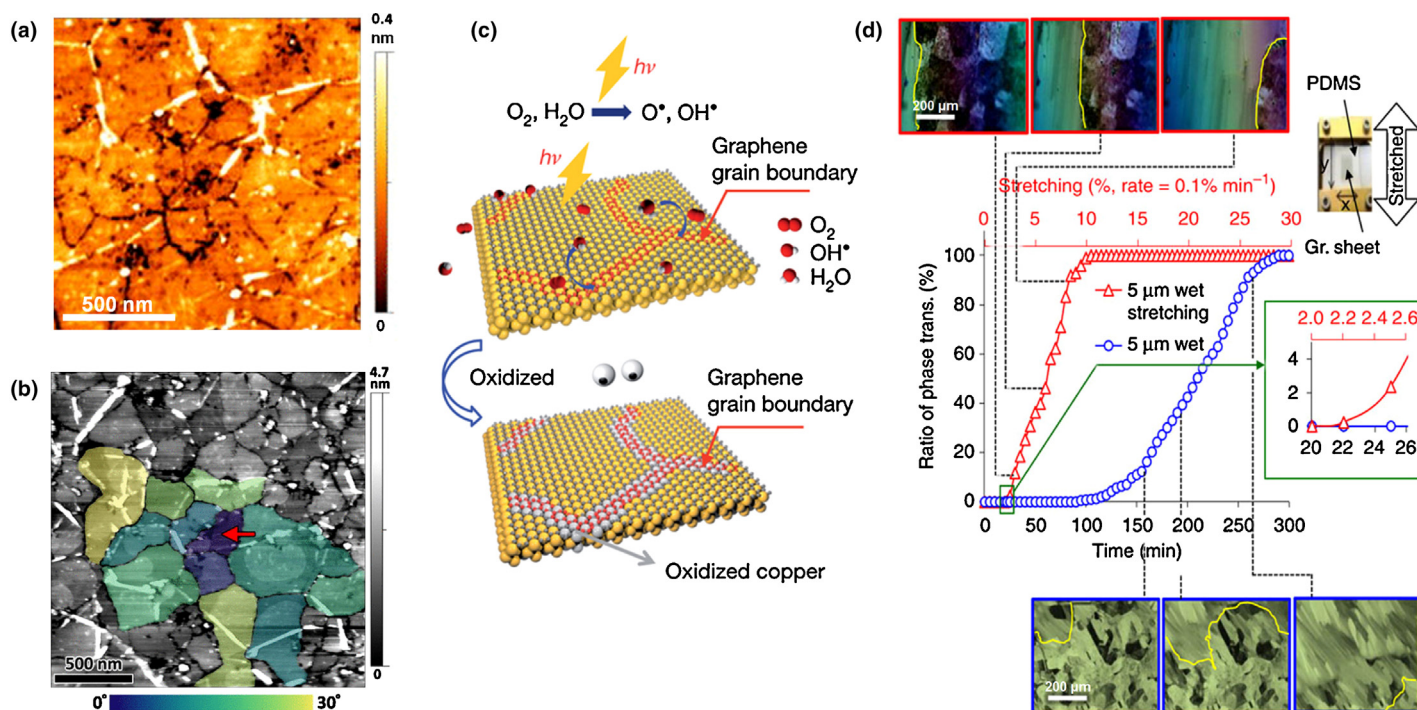


FIGURE 6

(a) CVD graphene on mica after oxidation; the black lines correspond to etch trenches. (b) Atomic-resolution image recorded by contact mode AFM on the grain indicated by the red arrow. (c) Diagram of the ultraviolet treatment of a graphene/Cu sample. The copper under the GBs was oxidized by radicals; the lines of oxidized copper broadened during continuing oxidation, thereby becoming visible using an optical microscope. (d) The variations in the phase transition ratio on the graphene/PDMS substrate during stretching of the graphene/PDMS substrate (red triangle) or in the absence of stretching (blue circle) and polarized optical microscope images of the LC phase transition. Adapted from Refs. [38,39,40].

nucleation mechanism involved in film growth by atomic layer deposition (ALD) [50]. Although a defect-free graphene without dangling bonds is chemically passive to ALD precursors [51], the dangling bonds in CVD graphene can naturally offer preferential nucleation sites for ALD. On the basis of this idea, they applied a few cycles of the ALD process to CVD graphene (Fig. 7a). As expected, the ALD materials primarily nucleated on defective sites (Fig. 7b and c). The reduction in the electrical sheet resistance with respect to the applied ALD cycles indicated that the defects were selectively healed. By proper selection of ALD materials, the resulting electrical and mechanical properties could be usefully adapted.

The additional extrinsic defects such as cracks are generated during the etching of Cu or Ni catalysts and the transfer process. In fact, these cracks cause a more serious degradation in the graphene properties than compared with structural defects such as GBs and atomic scale vacancies. It is particularly necessary to employ a new method for maintaining the graphene properties under high external strain for the utilization of CVD graphene in flexible, stretchable and wearable electronics. Won et al. reported a method of stacking CVD graphene sheets to improve the electromechanical properties, in particular, the stretchability (the value of engineering strain at which the electrical resistance starts to exceed a predefined limit during the electromechanical tensile test). [52]. Figure 8a shows illustrations of single- and double-layered graphene transferred to polyethylene terephthalate (PET) substrates. When tensile strain was applied to single-layer graphene, the electrical resistance of graphene rapidly increased only at a rate of 0.6% because the present cracks could propagate at this small

strain (Fig. 8b). By contrast, double- and triple-layer graphene endured more strain because the lower graphene layer transmitted the strain to the upper graphene layer with a large loss, resulting in interlayer sliding and consequently led to a different crack density between the lower and upper layers. Moreover, the upper layer covered the defects of the lower layer and provided an electrical current path, whereas the lower layer helped the upper layer exhibit its intrinsic properties by acting as a protector from the negative effects of the PET substrate, such as surface roughness and present chemical molecules. A smaller crack density, an additional current path and a screening effect of double-layer graphene can expand the range of available tensile strain.

The good mechanical characteristics of multilayer-stacked CVD graphene enable integration onto soft substrates, such as plastic or rubber, which are generally incompatible with conventional inorganic materials. Various flexible, stretchable and conformable devices have been successfully demonstrated. Figure 9a shows a graphene transistor on highly stretchable and deformable substrates such as rubber balloons. The transistor exhibits stable device performance during the volume expansion of the balloon [53]. Han et al. demonstrated a flexible, white, organic lighting-emitting diode (OLED) using multilayer-stacked graphene electrodes, which displayed superior performance compared with equivalent OLEDs containing an indium tin oxide electrode (Fig. 9b) [54]. Recently, graphene transistors and touch sensors conformably integrated on animal hides with rough surfaces were demonstrated. These graphene-based conformal devices exhibited stable electric characteristics, even under repetitive bending and twisting

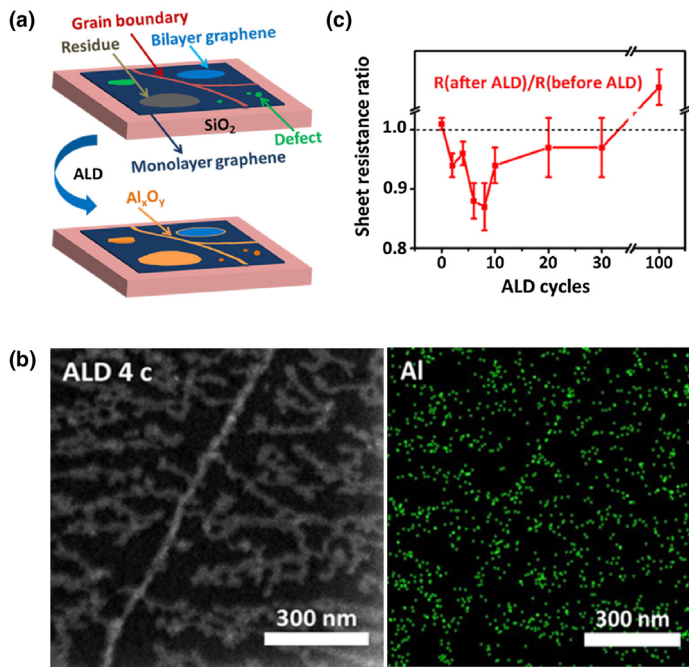


FIGURE 7

ALD-based defect healing process. (a) Diagram depicting the anticipated effects by ALD treatment on CVD graphene. For the Al_2O_3 ALD, trimethylaluminum (TMA, $\text{Al}_2(\text{CH}_3)_6$) and H_2O precursors were used. (b) Dark field transmission electron microscope (TEM) image of CVD graphene treated with 4 cycles of Al_2O_3 and the corresponding TEM-EDX (energy dispersive X-ray spectroscopy) elemental mapping of Al. (c) Electrical sheet resistance ratio of graphene before and after ALD treatment. Because nucleation and growth of Al_2O_3 on the graphene during ALD are highly dependent on the reaction of the surface species with the gas phase precursors used (TMA and H_2O), the surface reactions continue until the initial graphene surface is completely converted to the insulating Al_2O_3 surface. As can be noticed from the sharp increase in sheet resistance, it was not until 100 cycles of ALD that Al_2O_3 covered the entire graphene surface. Adapted from Ref. [50].

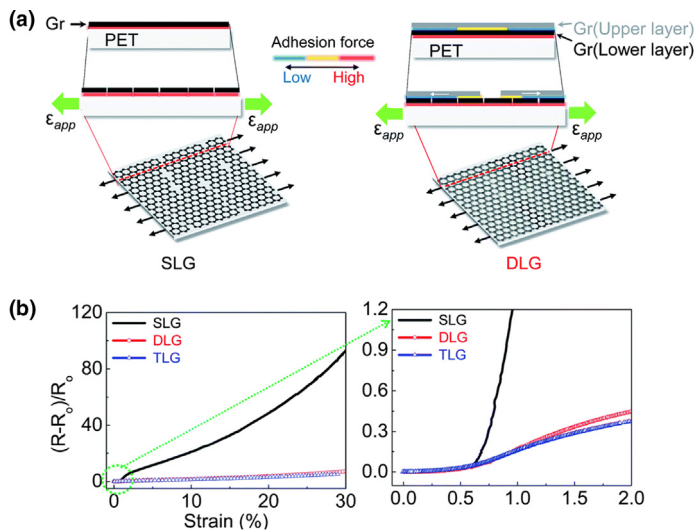


FIGURE 8

(a) Illustrations of SLG and DLG on PET. (b) Normalized changes in the electrical resistance of SLG, DLG and TLG with an applied tensile strain (SLG: single-layer graphene, DLG: double-layer graphene and TLG: triple-layer graphene). Adapted from Ref. [52].

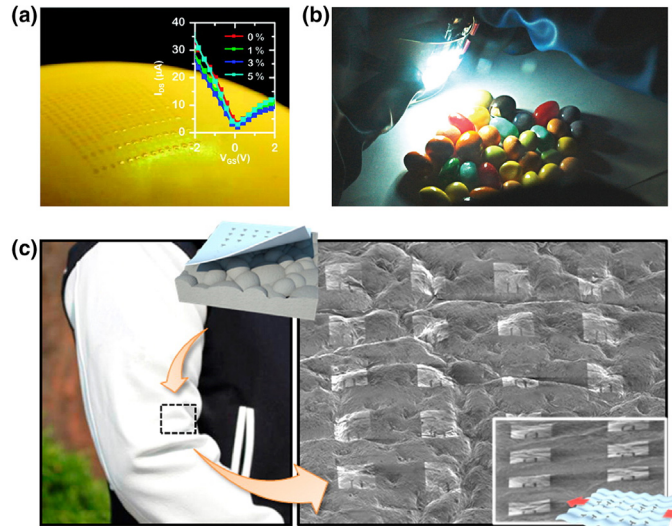


FIGURE 9

(a) Stretchable graphene-based transistor on the surface of a rubber balloon. (b) Flexible OLED solid-state lighting enabled with multilayered graphene electrodes. (c) Graphene-based conformal devices fabricated on the surface of an animal hide. Adapted from Refs. [53–55].

(Fig. 9c) [55]. These results confirm that graphene could be used to make a wide range of flexible and wearable electronic devices. However, the stretchability ($\sim 5\%$) in the reported graphene-based devices is still insufficient. Therefore, a variety of methods to minimize the defect density of graphene and to heal the created defects should be developed for expanding its stretchability range.

Conclusions and perspectives

Investigations of carbon over the past half century have left endless aftertastes, challenges and skepticism. Nevertheless, the promise of graphene has generated considerable interest among scientists and engineers. In fact, graphene has provided many opportunities for discovering new phenomena, and today it is regarded as a *treasure island* of condensed matter physics. However, many graphene researchers still retain a skeptical view concerning its commercialization. Any useful gadget in daily life must have mechanical stability for practical use. It is an essential prerequisite for graphene as well, without exception. However, despite its crucial significance, the current graphene studies concerning its mechanical limitations and efforts to overcome these limitations are eclipsed by other fields. The amount of papers dealing with these issues is fewer than ever. In this short review, the types of defect in CVD graphene generated during the growth and transfer/handling stages have been described. Fracture characteristics of graphene in the presence of defects have also been explored. In particular, it is important to be aware that defective graphene undergoes unwelcome abrupt failures by SCC in environmental conditions. Several recent methods for effective early detection of nano- and micro-sized defects present in graphene have also been summarized. Rather than the direct observation of defects on a small scale using time-consuming microscopic tools, indirect observation on a large scale using LC molecules appears to be technologically advantageous. Recent approaches to overcome the limited mechanical properties through selective defect healing by vapor phase treatment and graphene stacking in the form of multilayers have also been introduced. These methods could

enhance favorable device performance and reliability to some extent. However, further efforts to solve current challenges, such as imperfection problems that frequently occur at the graphene/metal interface [56], are still needed before the first appearance of graphene-based flexible and wearable electronic devices can be realized in the market.

Acknowledgements

S.-M.L. and J.-H.K. greatly acknowledge financial support by the Center for Advanced Meta-Materials funded by the Ministry of Science, ICT & Future Planning of Korea as Global Frontier Project (CMM-No. 2014063701, 2014063700) and by the Research Program of Korea Institute of Machinery & Materials (SC 1090). J.-H.A. acknowledges financial support by the Research Program (2012R1A2A1A03006049 and 2009-0083540) through the National Research Foundation of Korea (NRF), funded by the Ministry of Science, ICT and Future Planning.

References

- [1] W.S. Wong, A. Salleo, *Flexible Electronics: Materials and Applications*, Springer, New York, 2009.
- [2] J.A. Rogers, T. Someya, Y. Huang, *Science* 327 (2010) 1603–1607.
- [3] K.S. Novoselov, et al. *Nature* 490 (2012) 192–200.
- [4] C. Yan, et al. *Nanoscale* 4 (2012) 4870–4882.
- [5] S.-H. Bae, et al. *ACS Nano* 7 (2013) 3130–3138.
- [6] P. Blake, et al. *Nano Lett.* 8 (2008) 1704–1708.
- [7] F. Bonaccorso, et al. *Nat. Photonics* 4 (2010) 611–622.
- [8] S. Bae, et al. *Nat. Nanotechnol.* 5 (2010) 574–578.
- [9] X. Li, et al. *Science* 324 (2009) 1312–1314.
- [10] A. Reina, et al. *Nano Lett.* 9 (2009) 30–35.
- [11] F. Banhart, J. Kotakoski, A.V. Krasheninnikov, *ACS Nano* 5 (2011) 26–41.
- [12] A. Zandiatashbar, et al. *Nat. Commun.* 5 (2014) 3186.
- [13] D. Hull, D.J. Bacon, *Introduction to Dislocations*, Butterworth-Heinemann, Oxford, 2011.
- [14] A.J. Stone, D.J. Wales, *Chem. Phys. Lett.* 128 (1986) 501–503.
- [15] M.H. Gass, et al. *Nat. Nanotechnol.* 3 (2008) 676–681.
- [16] A.J. Lu, B.C. Pan, *Phys. Rev. Lett.* 92 (2004) 105504.
- [17] A. Hashimoto, et al. *Nature* 430 (2004) 870–873.
- [18] J. Červenka, et al. *Nat. Phys.* 5 (2009) 840–844.
- [19] P.Y. Huang, et al. *Nature* 469 (2011) 389–392.
- [20] J. Coraux, et al. *Nano Lett.* 8 (2008) 565–570.
- [21] J. Lahiri, et al. *Nat. Nanotechnol.* 5 (2010) 326–329.
- [22] A. Dahal, M. Batzill, *Nanoscale* 6 (2014) 2548–2562.
- [23] A.W. Tseng, et al. *Science* 336 (2012) 1143–1146.
- [24] C. Lee, et al. *Science* 321 (2008) 385–388.
- [25] G.H. Lee, et al. *Science* 3402 (2013) 1073–1076.
- [26] P. Zhang, et al. *Nat. Commun.* 5 (2014) 3782.
- [27] Y. Hwangbo, et al. *Sci. Rep.* 4 (2014) 4439.
- [28] S.M. Wiederhorn, *J. Am. Ceram. Soc.* 50 (1967) 407–414.
- [29] S.M. Wiederhorn, et al. *J. Mater. Sci.* 17 (1982) 3460–3478.
- [30] A. Salehi-Khojin, et al. *Adv. Mater.* 24 (2012) 53–57.
- [31] F. Schedin, et al. *Nat. Mater.* 6 (2007) 652–655.
- [32] O. Leenaerts, et al. *Phys. Rev. B* 77 (2008) 125416.
- [33] M. Topsakal, et al. *Appl. Phys. Lett.* 96 (2010) 091912.
- [34] H.C. Schniepp, et al. *J. Phys. Chem. B* 110 (2006) 8535–8539.
- [35] A. Ferrari, et al. *Phys. Rev. Lett.* 97 (2006) 187401.
- [36] K. Kim, et al. *ACS Nano* 5 (2011) 2142–2146.
- [37] L. Tapasztó, et al. *Appl. Phys. Lett.* 100 (2012) 053114.
- [38] P. Nemes-Incze, et al. *Appl. Phys. Lett.* 99 (2011) 023104.
- [39] D.L. Duong, et al. *Nature* 490 (2012) 235–239.
- [40] J.-H. Son, et al. *Nat. Commun.* 5 (2014) 3484.
- [41] D.W. Kim, et al. *Nat. Nanotechnol.* 7 (2012) 29–34.
- [42] S. Chen, et al. *Adv. Mater.* 25 (2013) 2062–2065.
- [43] C. Wang, et al. *Sci. Rep.* 4 (2014) 4537.
- [44] Y. Hao, et al. *Science* 342 (2013) 720–723.
- [45] J.-H. Kim, et al. *Science* 344 (2014) 286–289.
- [46] J. Song, et al. *Nat. Nanotechnol.* 8 (2013) 356–362.
- [47] D.-Y. Wang, et al. *Adv. Mater.* 25 (2013) 4521–4526.
- [48] S. Karoui, et al. *ACS Nano* 4 (2010) 6114–6120.
- [49] B. Wang, S.T. Pantelides, *Phys. Rev. B* 83 (2011) 245403.
- [50] D.V. Lam, et al. *Nanoscale* 6 (2014) 5639–5644.
- [51] X. Wang, et al. *J. Am. Chem. Soc.* 130 (2008) 8152–8153.
- [52] S. Won, et al. *Nanoscale* 6 (2014) 6057–6064.
- [53] S.-K. Lee, et al. *Nano Lett.* 11 (2011) 4642–4646.
- [54] T.-H. Han, et al. *Nat. Photonics* 6 (2012) 105–110.
- [55] Y.J. Park, et al. *ACS Nano* 8 (2014) 7655–7662.
- [56] F. Xia, et al. *Nat. Nanotechnol.* 6 (2011) 179–184.